Quantum size effect observed in ultrafine magnesium particles

Keisaku Kimura and Shunji Bandow
Instrument Center, Institute for Molecular Science, Okazaki-shi, Aichi 444, Japan
(Received 27 April 1987)

The static magnetic susceptibilities of ultrafine Mg particles were measured as a function of particle diameter in the temperature range from 2 to 240 K. The temperature-independent paramagnetism enhancement was observed and found to be inversely proportional to the cube of particle size, revealing for the first time direct evidence for the zero-dimensional magnetism in a small metal particle. The importance of the electronic state of corner atoms of a particle is suggested for this zero dimensionality. It was also suggested that this enhanced paramagnetism exhibits a phase transition at 150 K. The marked decrease in magnetic susceptibility at low temperature with the onset of moderate increase in intermediate temperature has been analyzed in terms of the quantum size effect. We first clarify experimentally the energy-level statistics of small metals by the combination of Poisson and orthogonal distributions. The effect of surface irregularity is discussed with the aid of Tanaka's formulas, which indicate that the surfaces of small particles are not rough. This is inconsistent with commonly accepted assumptions.

I. INTRODUCTION

The electronic state of small metal particles is characterized by the quantum size effect[1] which shows the development of the physical properties of materials from metallic to insulator at low temperature. This phenomenon is prescribed by energy-level statistics of electronic states of conduction electrons in small particles. For bulk metals, electronic energy levels form energy bands, justifying the one-electron-orbital picture with continuous k values. This picture is a consequence of the Bloch theorem and the use of Fermi statistics for conduction electrons. On the other hand, for small metal particles one cannot utilize Fermi statistics due to the constraint of electric neutrality for the electron distribution. Therefore the kind of energy-level statistics to be adopted is a key issue in these systems. The level statistics so far proposed in ultrafine particles (UFP's) are Poisson, orthogonal, and symplectic cases and these were used to derive the magnetic susceptibility and the specific heat of metal UFP's. However, there is a lack of direct experiments which are sufficient to give the details of level statistics, as seen in the recent review by Halperin.[2] Clarification of the basic character of level statistics is, hence, desirable to promote our understanding of *mesoscale* physics. Recently the present authors have reported new findings in the static magnetic susceptibility of small magnesium particles.[3] We found that there was a size-dependent paramagnetic enhancement superimposed on the quantum size effect at low temperature and on moderate increase in paramagnetism at intermediate temperatures. This slight increase was also found in the previous report[4] but has not yet been well clarified.

In this paper we analyze more precisely these peculiar phenomena found in Mg UFP's based on a level statistics incorporating the effect of surface irregularity presented by Tanaka and Sugano.[5] They found that the exponent of level repulsion deviated from unity to zero; that is, the level statistics changed from orthogonal to Poisson, depending on surface irregularity. The size-dependent paramagnetic enhancement is also analyzed in this report and is found to be a zero-dimensional phenomenon.

Magnesium has been selected as a sample for four reasons.

(1) Mg, as a representative of divalent metals, gives even-electron particles, the magnetic susceptibility of which displays no increase in the low-temperature region according to the quantum size effect if electric neutrality holds. Therefore we can accurately distinguish this from an exogenous spin effect on the magnetic susceptibility which follows a Curie law. An odd-electron system exhibiting the quantum size effect also follows the Curie law or Curie-Weiss law. It is therefore difficult to distinguish the true quantum size effect (volume effect) from the behavior due to contaminated spins at the surface (surface effect). Namely, the quantum size effect manifests itself more distinctly in an even-electron system.

(2) The bulk magnetic susceptibility of Mg shows paramagnetism, revealing that the spin paramagnetism is greater than other diamagnetic contributions. We expect, therefore, a dramatic decrease in the Pauli paramagnetism of a Mg UFP in the low-temperature region. Consequently, it will be easy to detect the size dependence of the quantum size effect.

(3) Spin-orbit coupling is weak in Mg, simplifying the interpretation of results.

(4) High-purity starting materials are available from commercial sources.

II. EXPERIMENT

In order to get a sharp particle size distribution, small metal particles were carefully prepared, resulting in a very small amount of particles requiring high-sensitivity measurements of the magnetic susceptibility. Careful attention was paid to sample handling to avoid air oxida-

 ©1988 The American Physical Society

tion throughout the experiments. Mg UFP's were prepared by the matrix isolation method combined with the gas evaporation technique described elsewhere.[6] Gaseous hexane was introduced *in vacuo* to a Pyrex Dewar cooled by liquid nitrogen to make the cryogenic matrix. A Mg tip (99.99%) was then sublimated in an atmosphere of 99.9999% He gas and the UFP's produced were trapped on the matrix of hexane. In order to avoid a particle contact problem, gaseous hexane was introduced again giving a new surface of the cryogenic hexane matrix. These procedures were repeated several times until a sufficient amount of particles was accumulated in the matrix for magnetic susceptibility measurements. After warming the Dewar at room temperature, nitrogen gas (purity greater than 99.9995%) was introduced to the Dewar. Through a SEPTA rubber cap, a colloidal solution containing Mg UFP's was then transferred to a storage bottle by a syringe with a metal Luer lock. Both a bottle and a syringe were completely flushed with high-purity nitrogen gas in advance. A sample solution for magnetic susceptibility measurements was transferred from a storage bottle to a quartz cell in a glove box. Hexane in the quartz cell was interchanged to the degassed paraffin liquid in an atmosphere of nitrogen or helium in a glove box. Paraffin liquid was effective in reducing oxidation and also particle clustering during the examination of a small tin particle system.[7] If particle clustering takes place, the diamagnetic susceptibility is largely enhanced through the Josephson contact between particles. We observed this enhancement in the deposited powders from solution and also in pressed discs but no enhancement was observed in the Sn particles in paraffin liquid. Therefore, at least, electron transfer through interparticle tunneling[8] is suppressed. Sample treatment and weighing were always conducted in a glove box. The size distribution of UFP's was determined directly from electron micrographs of the samples prepared by dropping the sample solution onto a Cu mesh covered with an evaporated carbon film. The size histogram was prepared by an image analyzer, KONTRON IBAS-1.

Magnetic susceptibility was measured by a high-sensitivity Faraday-type magnetic balance unit with a superconducting magnet and with a microprocessor-aided data logging system. The force loaded on the sample was measured by a Cahn RG electrobalance with the accuracy of 10^{-6} g. A separate magnet unit, composed of a main coil (an operating magnetic field was set at 1 T during the measurements of magnetic susceptibilities) and a pair of reverse Helmholtz coils for the field gradient (5 T/m), was used to ensure absolute magnetic susceptibility measurements. The main field and the field gradient were calibrated by a GaAs Hall device. The force due to the shift of the magnetic center was 20 μg at most.[9] A platinum-resistance thermometer was used to read temperatures higher than 25 K and a carbon-resistance thermometer for lower temperatures. These temperature readings were calibrated in the whole temperature range with a magnetic thermometer with the use of paramagnetic $Cr(NH_3)_6Cl_3$ salt at the sample position. The accuracy of the temperature was checked against the superconducting transition temperatures of Nb and Pb. As described in a previous paper,[10] the spin state of organic radicals of only 18 μg was determined by our high-sensitivity system. A sample (typically 5-mg Mg UFP's in 100 μl paraffin liquid) in a cylindrical Suprasil-grade quartz cell was suspended by a 0.2-mm-diam quartz fiber from the arm of an electrobalance in a He gas stream atmosphere. Then the samples were rapidly frozen at about 100 K in a cryostat and evacuated by a diffusion pump for 1 h to remove oxygen completely, and the samples were gradually cooled to 4.2 K under a helium atmosphere (10^3 Pa). Measurements were carried out in the temperature range from 2 to 240 K. Control experiments were performed using the same quartz cell carrying the same amount of paraffin liquid within 50 μg weight difference immediately after or before the measurement for each sample. The magnetic susceptibilities of the samples were obtained after subtracting the control values. No ferromagnetic impurities were detected in the samples measured at 4.2 K, as was indicated by the field dependence of the magnetization up to 5 T.

Sample characterization was done both by x-ray diffraction and by x-ray photoelectron spectroscopy (XPS). After measurement of magnetic susceptibility, a sample of 5.2-nm particles was exposed to air and a Cu $K\alpha$ x-ray powder diffraction was taken under aerobic conditions. The surface of another 3-nm Mg UFP sample was analyzed by XPS prepared under the same conditions but without paraffin liquid.

III. RESULTS

The x-ray diffraction trace showed only four strong metal Mg peaks, in addition to one very broad pattern of amorphous MgO in the 2θ range from 50° to 30°. We concluded that the MgO was distributed over the surface of the Mg UFP and that about 20% of total Mg atoms were oxidized, on the basis of the ratio of the peak areas of Mg to MgO. Since analysis was conducted under aerobic conditions after magnetic susceptibility measurements, most of the oxygen seen by x-ray diffraction was introduced after the measurements. The XPS spectra showed that half of the surface Mg atoms were oxidized. Therefore oxidation of half of the surface (25% oxidation of total atoms for 3-nm particles and 16% oxidation for 5.2-nm particles) is consistent with the observed value (20% oxidation) by x-ray diffraction. We can estimate the diamagnetic contribution from oxidation to the magnetic susceptibility as follows:

$$\chi_{\text{obs}}=(1-f_{\text{oxidation}}/100)\chi_{\text{Mg}}+(f_{\text{oxidation}}/100)\chi_{\text{MgO}} . \tag{1}$$

Here χ_{obs} is an apparent magnetic susceptibility (sum of metal Mg and MgO), $f_{\text{oxidation}}$ is the percentage of the total Mg atom oxidized, and χ_{Mg} is the susceptibility of a metallic part. Using the value of oxidation of 20% and χ_{MgO} being -0.25×10^{-6} emu/g,[11] we get

$$\chi_{\text{Mg}}\sim 1.25\chi_{\text{obs}} . \tag{2}$$

The correction factor 1.25 is a maximum value because of an overestimate of the percentage oxidation of Mg (true

correction factor lies between 1.25 and 1.00). However, this calculation is appropriate for the oxidized samples after magnetic measurements, whereas the actual samples hardly suffer from oxidation. Therefore no correction was made for magnetic susceptibilities measured throughout in this paper.

We have measured five kinds of particles, the average diameters of which were 40 nm (a size distribution half-width of 50 nm), 5.2 nm (5.8 nm), 2.5 nm (1.6 nm), 1.7 nm (0.6 nm), and 1.4 nm (0.6 nm), respectively. It is apparent that the smaller the particle size, the narrower is the distribution. As an example, the size distribution of the smallest particle is shown in Fig. 1, which gives a sharp distribution with a half-width of 0.6 nm. Figure 2 shows the temperature dependence of the mass magnetic susceptibilities (emu/g) of these samples. The plots for 2.5-nm particles were omitted in this figure to avoid overlapping with the points for particles of other diameters. Exogenous paramagnetic species (odd spins) were checked by ESR at 2 K and were found to be less than 1×10^{-7} emu/g at this temperature. Therefore odd spin particles and species did not contribute to the static magnetic susceptibility for the whole region measured. The largest particles ($D=40$ nm) yielded a constant paramagnetic susceptibility, $\chi_b=0.68\times10^{-6}$ emu/g, comparable to the bulk value reported (0.55×10^{-6} emu/g).[12] No increase in magnetic susceptibility was observed in the low-temperature region in this sample, reaffirming the ESR datum which showed contribution from paramagnetic impurities to be less than 1×10^{-7} emu/g at the lowest temperature. A constant Pauli paramagnetism, characteristic of the bulk metal, was observed only in this sample, in sharp contrast to the smaller size particles that showed an anomalous temperature dependence, as seen in Fig. 2. For smaller particles, we note a striking enhancement of the magnetic susceptibility in the higher-temperature region and a sudden decrease in the lower-temperature region with the onset of a slight increase in the middle-temperature region. A decrease in magnetic susceptibility at very low temperature is known as the quantum size effect[1] and we have reported, for the first time, observation of this effect in the static magnetic susceptibility of small Mg particles in a previous paper.[4] The slight increase of the magnetic susceptibility in the intermediate-temperature region, remarkable in smaller particles, was also noticed in our previous report but cannot be explained by the existing theory. In Sec. V we will analyze this behavior based on a new model we propose in this paper, which shows that these findings are also merely a manifestation of the quantum size effect.

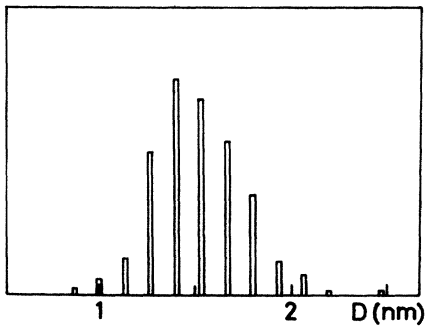

FIG. 1. Size distribution in the smallest sample of Mg particles. The majority at 1.4 nm contains approximately 60 atoms in a particle. The full width at half maximum is about 0.6 nm.

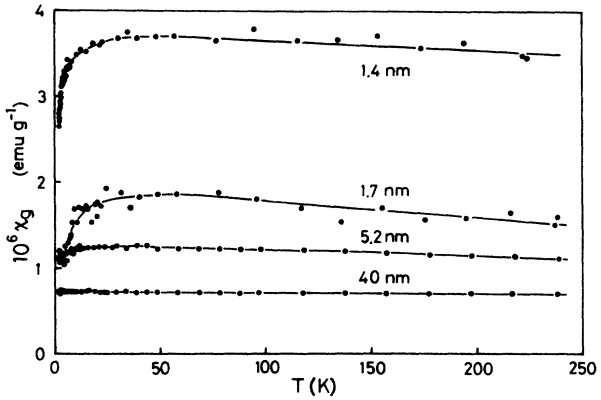

FIG. 2. Magnetic susceptibilities of Mg UFP's as a function of temperature. Numbers in nm stand for average diameters of UFP's determined by electron micrograph. Plots of the 2.5-nm particles were omitted in this figure because of overcrowding of points for particles of other diameters.

First we focus our attention on the marked paramagnetic enhancement at high temperature where it seems to be constant above 150 K. We define this constant susceptibility ($\chi_{\rm UFP}$) as the mass magnetic susceptibility of Mg particles at 240 K. Figure 3 shows the constant paramagnetic susceptibility normalized to the bulk value (χ_b) as a function of the inverse of the number of atoms

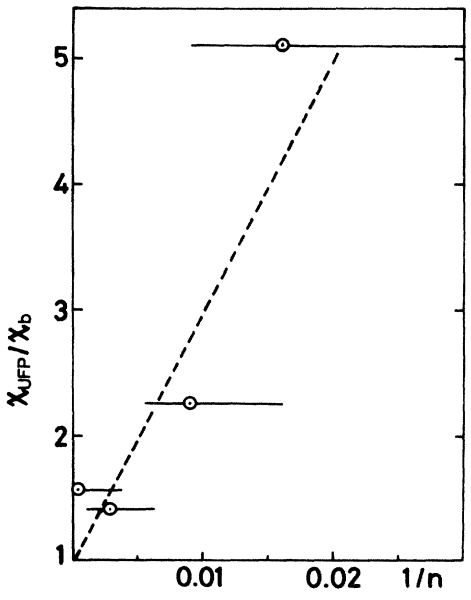

FIG. 3. Normalized magnetic susceptibilities of UFP's as a function of the inverse of the number of atoms in a particle. $\chi_{\rm UFP}$ is a mass magnetic susceptibility at 240 K. Horizontal bars in the figure reflect the particle size distribution. A dashed line stands for the relationship of $\chi_{\rm UFP}$ being inversely proportional to the number of atoms in a particle.

in a particle. From this figure, we can deduce an empirical relationship between the number of atoms in a particle and χ_{UFP}, although our results are approximate and the data are rather scattered because of the difficulty in controlling the distribution of particle diameters (size distribution is represented by a horizontal error bar in the figure). The empirical relationship is given by

$$\chi_{\mathrm{UFP}}=\chi_b+\mathrm{const}\times\chi_b/n \ . \tag{3}$$

Here, the constant in the second term was found to be 200 ± 50. This relationship is insensitive to the temperature at which we define χ_{UFP}, e.g., 100 instead of 240 K, because the enhancement is larger than the differences in magnetic susceptibilities at different temperatures in the high-temperature range. Since the contribution of diamagnetism due to Mg ions to the magnetic susceptibility is independent of particle size, the above relation can be rewritten in terms of contribution from conduction electrons only, i.e.,

$$\chi^e_{\mathrm{UFP}}=\chi^e_b+\mathrm{const}/n \ . \tag{4}$$

Returning now to Fig. 2 it seems that the enhanced paramagnetic susceptibility consists of two components; one is a temperature-independent term which contributes to the observed dramatic increase in magnetic susceptibility. The other determines the temperature profile of magnetic susceptibility in the low-temperature region, which approaches zero when the temperature decreases. The analysis of these components is treated in Sec. V.

IV. THEORETICAL REMARKS

The level separation problem in small metallic particles was considered by Kubo[1] and Fröhlich.[13] Later the energy-level statistics were treated as a random-matrix problem by Gor'kov and Eliashberg,[14] and were applied to the spin susceptibility by Denton *et al.*[15] Figure 4 shows the results of Denton *et al.* for the case of even-electron particles where temperature is normalized to the average level splitting at the Fermi level. The random-matrix ensemble is orthogonal ($\omega=1$) when the spin-orbit coupling of conduction electrons is weak and time-reversal invariance holds. The ensemble is symplectic

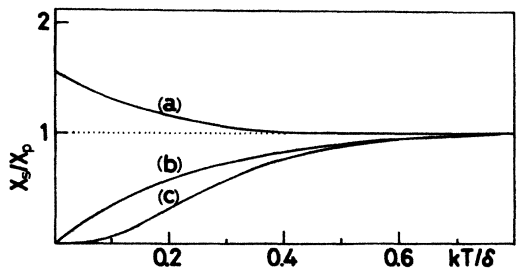

FIG. 4. Temperature dependence of spin susceptibilities of even-electron particles for several level statistics after Denton *et al.* (Ref. 15). (a) Poisson case (random eigenvalues for the diagonal matrix elements; $\omega=0$), (b) orthogonal case ($\omega=1$), and (c) symplectic case ($\omega=4$). All values are normalized to the Pauli value taken to be $\chi_P=2\mu_B^2/\delta$, where δ is the average level splitting at the Fermi level and μ_B is the Bohr magneton.

($\omega=4$) when the spin-orbit coupling is strong and time-reversal invariance holds. The exponent ω governs the behavior of the spin susceptibility of small metal particles at low temperature, i.e., $\chi_s\propto(kT/\delta)^{\omega}$. It is believed that the Poisson distribution ($\omega=0$) originally presented by Kubo is not correct because the effect of energy-level repulsion was left out in his treatment. However, the recent study by Tanaka and Sugano[5] has revealed that the exponent ω characterizing the degree of level repulsion strongly correlates with the roughness of the particle surface such that ω shifts from 1.0 (orthogonal case) to 0 (Poisson case) decreasing with surface irregularity where the orthogonal distribution is approximated by Wigner ones. Generalization of the level spacing distribution was successfully achieved with the use of the Brody distribution, which is devised as an interpolation formula connecting Wigner and Poisson distributions at both limits. Therefore we need to reformulate the theory of the quantum size effect to which the surface effect must be explicitly included. This effect is greatly enhanced in UFP's as shown in the present study. Unfortunately, there is no theory on the magnetic susceptibility based on a level statistics incorporating the surface effect. However, we can take account of this contribution as follows. Since the spin-orbit coupling is very small in Mg and since the static magnetic susceptibility is defined in the weak limit of magnetic field, we can accept the orthogonal ensemble [case (b) in Fig. 4] as a starting distribution on which the Poisson contribution [case (a) in Fig. 4] is superimposed in order to include the deviation of ω from 1 owing to the reduction of surface roughness.

We will propose here that the spin susceptibility of small Mg particles with noninteger ω is represented by the combination of the magnetic susceptibilities for the Poisson and orthogonal cases as follows:

$$\chi_s(\omega)=\chi_0^{1-\omega}\chi_1^{\omega} \ , \tag{5}$$

where χ_0 is a magnetic susceptibility for the Poisson level distribution and χ_1 is for the orthogonal case. Hence this magnetic susceptibility connects two limiting cases such that χ_s coincides with χ_0 for $\omega=0$ and with χ_1 for $\omega=1$. In Fig. 5, the magnetic susceptibilites (in the unit of χ_P) thus defined are displayed for several noninteger values ω, where the magnetic susceptibility is plotted as a function of the logarithm of the absolute temperature in order to present behavior over a wide temperature range. It is now instructive to discuss features of these curves as functions of ω and temperature. The magnetic susceptibility χ_s for particles with a given size with $\omega=0.1-0.3$ decreases at around $kT/\delta\sim0.5$ and then it modestly increases at about 0.1–0.2, followed by a sudden decrease when the temperature decreases. There are a maximum and a minimum in the temperature profile of the spin susceptibility, quite different from those in the orthogonal and Poisson cases where the curves are monotonously decreasing or increasing with temperature. For large particles we can observe the magnetic susceptibility only in the large kT/δ region, e.g., larger than 0.5, while we can follow the whole kT/δ region in the figure, for example, from 0.005 to 0.5 for small particles with large δ. For

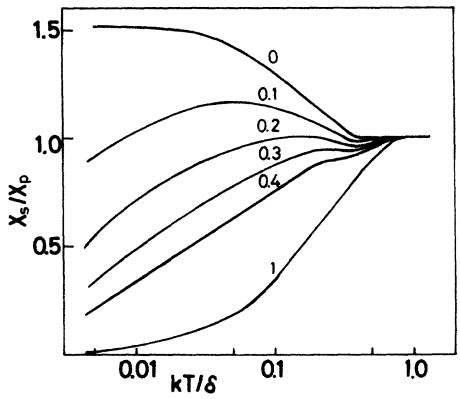

FIG. 5. Spin susceptibilities of even-electron particles for a noninteger exponent ω as a function of logarithm of absolute temperature. The numbers in the figure show the exponent ω. $\omega=0$, Poisson case [case (a) in Fig. 4]. $\omega=1$, orthogonal [case (b) in Fig. 4], and others are calculated from Eq. (5). Note that temperature is expressed in logarithmic units.

particles with $\omega=0.1-0.4$, we notice that the decrease in χ_s is obvious at $kT=\delta/2$. This gives a rough estimate of δ from the behavior of the spin susceptibility for each ensemble of particles. Finally, we will point out that the quantum size effect can be easily and clearly observed if we use particles with irregular surfaces ($\omega=1$) as seen in Fig. 5, line 1.

V. DATA ANALYSES

In order to compare the experimental results with the theoretical spin susceptibility, we must extract the term of spin only magnetism from the data and this can be done with the following procedures. As described in Sec. III, the observed magnetic susceptibility consists of two components, temperature-dependent and -independent terms. In the case of small Mg particles, the magnetic susceptibility can be divided as follows:

$$\chi_g=\chi_{\text{ion}}+\chi_{\text{orb}}+\chi_s+\chi_{\text{enh}}\ , \tag{6}$$

where the first term in the right-hand side stands for the diamagnetism of the Mg^{2+} ion, the second for orbital contribution, the third for spin susceptibility, and the last term represents the paramagnetic enhancement observed only in small particles and approximately expressed as const/n in Eq. (3). The first three terms in Eq. (6), therefore, should be equal to χ_b in the high-temperature limit. We assume that the terms χ_{ion}, χ_{orb}, and χ_{enh} do not depend on temperature and that only χ_s is the origin of the observed temperature dependence. Using the experimental value of $\chi_{\text{ion}}=-0.18\times10^{-6}$ emu/g,[16] the calculated value for $\chi_{\text{orb}}=-0.105\times10^{-6}$ emu/g,[17] and χ_{enh} determined in Eq. (3), we obtained χ_s for each sample of particles. The χ_s thus derived has an ambiguity due to the estimation of χ_{enh} and also to the use of a calculated value of χ_{orb}. However, in order to compare χ_s with the theoretical value, it is sufficient to consider the temperature dependence of χ_s, and we need not compare their absolute values. Absolute values in the units of the Pauli paramagnetic susceptibility at 100 K are 1.5, 1.4, and 1.2 for 5.2-, 2.5-, and 1.4-nm particles, respectively. Errors are larger for large particles, because the size distribution is very broad for large particles. Therefore we normalized the χ_s values calculated to the value at 100 K, represented as χ_n^s, and these are shown in Fig. 6 where the datum of 1.7-nm particles is omitted, because of a technical problem encountered for this sample and lack of an accurate control experiment for this sample. As seen in Fig. 2, the large scattering of the measured points for the 1.7-nm particles at lower temperatures reflects this problem. The data for the 1.7-nm sample in Fig. 2 were obtained from the subtraction of a cell blank by using our earlier data for this cell since direct control experiments just after each measurement of the samples was not possible at this time. Errors are larger in the low-temperature region but they are smaller at high temperatures. This result assures the validity of the results for the 1.7-nm particles at high temperatures. In Figs. 6(a)–6(c), the χ_n^s plots thus obtained are shown in addition to the curves calculated using Eq. (5). Some remarks should be made here. Figure 6(a) shows plots of χ_n^s values for the 5.2-nm particles where a decrease in magnetic susceptibility is obvious at 8 K, corresponding to half of the calculated δ from the size of particles, consistent with the prediction in Sec. IV. The calculated curve was obtained with $\omega=0.3$ and $\delta=15$ K. This corresponds to the large kT/δ region in Fig. 5. The magnetic susceptibility of the 5.2-nm particles decreases with decreasing temperature through a minimum point at 5 K. We also notice that a decrease in magnetic susceptibility is again found at high temperatures, beginning at around 150 K, and this behavior is also common to the other particle samples.

In Fig. 6(b), where the χ_n^s values for the 2.5-nm particles are plotted, one minimum at 100 K and one maximum at 50 K are evident. The measured temperature range exceeds 10^2 and covers the whole range in Fig. 5. The decrease in magnetic susceptibility at higher temperature is the same as the case for the 5.2-nm particles. The calculated curve is obtained by using $\omega=0.2$ and $\delta=300$ K. Figure 6(c) shows the χ_n^s values for 1.4-nm particles where a maximum at around 150 K is evident. Note that the decrease in the higher-temperature region is large in these particles. The overall features are well expressed by the calculated curve with $\omega=0.2$ and $\delta=800$ K. Because of the large δ, we can observe only the small kT/δ region for this particle. In Table I, we summarize all the fitting parameters thus given, where δ_D is the calculated level splitting at the Fermi level ε_F ($=7.0$ eV) using the following equation:

$$\begin{aligned}\delta_D&=1/D(\varepsilon_F)\\&=4\varepsilon_F/3N\ .\end{aligned}\tag{7}$$

Here, $D(\varepsilon_F)$ is the density of states at the Fermi level and N stands for the number of conduction electrons in a particle which was determined by the particle size. The other two parameters in Table I, δ and ω, are determined by fitting to Eq. (5). As will be mentioned later, δ and ω are not merely fitting parameters but have physical bases

supported from other observations. A small value of ω indicates that the level distribution is close to the Poisson case. Agreement between the level splitting calculated by the particle size, δ_D, and that by curve fitting, δ, justifies our model and the treatment based on Eq. (5).

VI. DISCUSSION

The observed paramagnetic enhancement at high temperature is expressed by Eq. (3), showing the second term

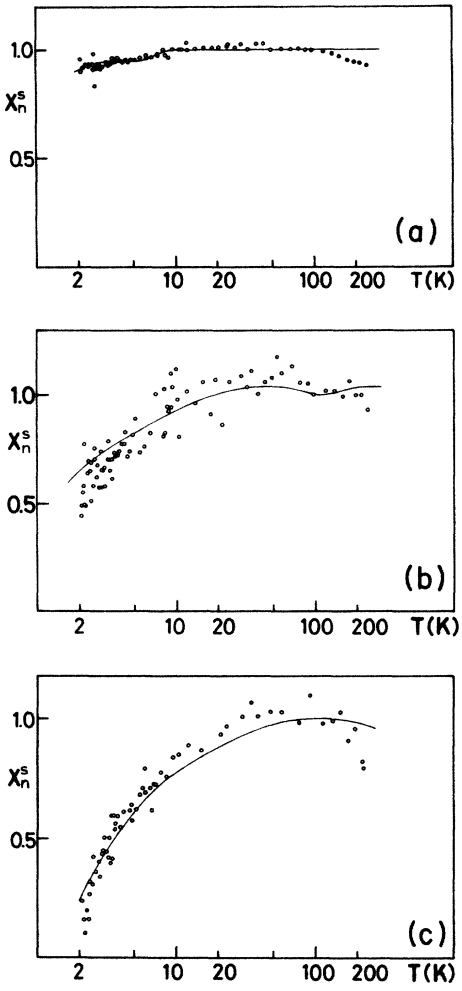

FIG. 6. Spin susceptibility of Mg UFP's as a function of temperature. The susceptibility is normalized to the value at 100 K. The solid lines are calculated from Eq. (5) in the text. Temperature is shown in logarithmic units. (a) Data for 5.2-nm particles. Calculated curve with $\omega=0.3$ and $\delta=15$ K. The value of χ_s in the unit of Pauli spin susceptibility (χ_P) is 1.5 at 100 K. The decrease in the susceptibility begins at 8 K, which is one-half of δ. The susceptibility decreases also prominently above 150 K. (b) Data for the 2.5-nm particles. Calculated curve with $\omega=0.2$ and $\delta=300$ K. The value of $\chi_s/\chi_P=1.4$ at 100 K. The amount of decrement at the low-temperature region is larger than that of the 5.2-nm particles. There are a minimum at around 100 and a maximum at 50 K. Spin susceptibility decreases again above 200 K. (c) Data for the 1.4-nm particles. Calculated curve with $\omega=0.2$ and $\delta=800$ K. The value of $\chi_s/\chi_P=1.2$ at 100 K. There is a maximum at 100 K. The decrease at low temperature is very large and it is also evident above 200 K.

TABLE I. Level splitting parameters found in Mg UFP's. δ_D is the average level splitting at the Fermi level calculated from particle size, δ the level splitting obtained from the fitting in Fig. 6, ω the level repulsion parameter obtained from the fitting in Fig. 6, and $\Delta\chi/\chi$ the deviation of χ_n^s from Eq. (5) at high temperature.

Sample diameter (nm)	δ_D (K)	δ (K)	ω	$\Delta\chi/\chi$
5.2	17	15	0.3	0.07
2.5	150	300	0.2	0.11
1.4	880	800	0.2	0.19

being inversely proportional to the volume. A physical quantity which depends on volume becomes size independent when normalized by volume or mass. The quantity depending on surface area is inversely proportional to the size when normalized to the volume. It will be inversely proportional to the volume if it is size independent and when it is normalized to the volume. Thus χ_{enh} is suggested to be size independent. The rather large error bars in Fig. 3 may lead to a question concerning the observed size dependence being $1/n^{1/3}$ for the surface contribution, because n is proportional to volume. However, we can examine the appropriateness of the fitting as follows. Assuming this size dependence being n^p, the plot of $\log(\chi_{\text{UFP}}/\chi_b-1)$ versus $\log n$ gives the exponent of n. Figure 7 shows this relation for the Mg UFP, along with the data on the Os polynuclear cluster complex studied in a previous paper.[3,18] The broken lines both in Os (line a) and Mg (line b) correspond to $p=-1$ [same as Eq. (3)] and the dash-dotted line in b is $p=-\frac{1}{3}$ as reference. Note that the size dependence of $1/n$ but not $1/n^{1/3}$ holds for both metals and for a very wide range of cluster size from four to more than 10^3 atoms. However, this finding presents a difficulty in explaining the novel size dependence, i.e., size independence or zero dimensionality.

Concerning the magnetic enhancement in small metal particles, there were reports on the small Cr (Ref. 19) and

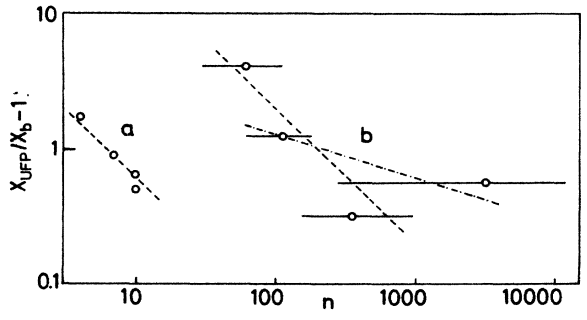

FIG. 7. Logarithmic plot of magnetic susceptibility at high temperature (χ_{UFP}) vs the number of atoms in a particle. The susceptibility is normalized to that of bulk value. (a) Osmium cluster complex after Kimura and Bandow (Ref. 3). (b) Mg UFP's in this study. Horizontal bars reflect the particle size distribution. The dashed lines in (a) and (b) represent the $1/n$ dependence. The dash-dotted line in (b) stands for the relation of the inverse of n to the $\frac{1}{3}$. Note that the number of atoms in a particle, n, covers a very wide range from four to over 1000.

V metal particles.[20] The magnetic enhancement found in these particles was interpreted as surface ferromagnetism in Cr particles[21] and as surface localized spins in V particles where the size dependence was expressed as $1/n^{1/3}$.[20] The observed magnetic moment per surface V atom, $2\mu_B$, was well explained by calculations taking into account the surface contribution, giving 2.4 μ_B per surface atom.[22] The observed size dependence of $1/n^{1/3}$ is completely compatible with this explanation as being due to a surface effect. However, we have found in Mg UFP's the unusual size dependence, $1/n$, suggesting that the origin of this phenomenon is size independent. Size-independent contributions to the measured magnetization might include the demagnetization effect, known in bulk ferromagnetism and in the perfect Meissner effect in superconductivity. However, a demagnetization effect for the weak magnetism in the present case is not likely. To explain the size-independent term, the topological symmetry of particles, such as the number of edges and corners of crystals, that affects the electronic state of metals may be considered. The ratio of the number of atoms at the corner to the total atoms amounts to about 20% in a 1.4-nm Mg hexagonal particle. The number of corner Os atoms is four, regardless of size in the Os cluster complexes.[18] If the particles have the same number of corner atoms independent of their size (topologically identical), then a size effect such as is observed in χ_{enh} might be expected. This means that the particle shape is not random. Therefore, our result is inconsistent with the basic assumptions of random-matrix theory on the surface potential of the UFP, that is, the surface of the UFP is random owing to uncontrollable surface shape. As for the origin of enhanced paramagnetism, we do not know much about what mechanism is responsible for the size-independent, i.e., zero-dimensional, small paramagnetism in the present case. Presumably, spin polarizations of corner atoms interact with each other mediated by conduction electrons, though this is a speculation and is not consistent with the result of a calculation of fcc metal clusters.[23] Concerning the factors determining the constant in the second term of the right-hand side of Eq. (3), the number of corner atoms and the interaction between them should be taken into account. Apparently our findings can be correlated to the phenomena found in "mesoscopical physics" recently proposed[24] and we need further understanding of the nature of this magnetism.

Both the experimental curve of spin susceptibility versus temperature which falls toward zero at very low temperature, and an apparent size dependence, prominent in smaller particles, are clearly predicted by the quantum size effect. Moreover, a slight increase in magnetic susceptibility observed at the intermediate-temperature region, which was not clarified in the previous report,[4] is also explained by taking into account the contribution from the shape of particles to the energy distribution. It is clear that the curve shown in Fig. 6 displays a typical quantum size effect and that the energy-level statistics follow the Brody distribution with the level repulsion parameter ω. From the fitting value of ω, we derive the roughness parameter R with Eq. (3.4) of Ref. 5, where R is defined as the ratio of the number of irregular sites to the particle size, and is normalized to zero if there is no irregularity.[25] The ω values in Table I show that R is only 3% and probably less for all the particles measured. This again affirms the fact that the particles are topologically equivalent, consistent with the result from the zero dimensionality of χ_{enh}. Namely, the surface of a Mg UFP is smoother than previously believed. This is why the energy-level statistics are characterized by the noninteger level repulsion exponent ω and why the magnetic susceptibility is given by the combination of magnetic susceptibility for Poisson and orthogonal cases. Therefore in the present case it is not adequate to assume random surface potentials for small metal particles. Instead we propose to treat the ensemble of topologically identical particles with the same number of atoms and the same roughness parameter in the theoretical consideration. As for the δ value in Table I, it is curious that we have good agreement between δ_D derived from the free-electron model with Fermi-Dirac distribution and δ from the Brody distribution. However, the density of states is insensitive to surface irregularity, as is stated in Tanaka's paper. It is reasonable, therefore, to get fairly good agreement in both distributions.

Here we should remark on the effect of the preparation method for UFP's on the surface irregularity, because the shape of the particles may depend strongly on the preparation methods. We employed the gas evaporation technique where UFP's grow in an isotropic three-dimensional free space. On the other hand, some experiments were performed using island crystal growth processes where UFP's grow on a two-dimensional substrate which is anisotropic at least along one axis. The difference in UFP preparation techniques and conditions may affect the particle shape as well as the surface irregularity. In the ensemble of particles with irregular surfaces where the level distribution approaches orthogonal, we expect a larger quantum size effect than the particles with regular surfaces, as stated in Sec. IV. At the same time, it is also expected that the enhancement of paramagnetism diminishes. Nonroughness of the surface of small particles in our sample was, though imperfectly, directly observed in a preliminary experiment by a high-resolution electron microscope in our laboratory. A recent report by Iijima with a real time electron microscope clearly shows a beautiful crystal habit in 2-nm Au particles.[26] It was also supported by the electron micrograph of Ag particles produced by the as evaporation technique.[27] We emphasize again that the surface of metal UFP's with sizes down to 1 nm is not irregular, contrary to the common assumption.

As mentioned in Sec. V, there is a systematic deviation in χ_n^s at high temperature. The observed χ_n^s is always smaller than the calculated value and this trend is greater for smaller particles. This deviation is also shown in Table I at the highest temperature measured in terms of its ratio to the calculated value of χ_n^s at the same temperature. Note that the ratio of this deviation has a clear size dependence. There is no reason that the spin paramagnetism of small metallic particles decreases at higher temperatures. We point out that the normalized spin susceptibility χ_n^s is derived from the assumption of

the constancy of χ_{ion}, χ_{orb}, and χ_{enh} in Eq. (6). Of these three terms, only χ_{enh} reveals a clear size dependence. If χ_{enh} changes at a certain critical temperature, this induces a change in χ_n^s in our calculation and this change automatically introduces the size dependence because χ_{enh} strongly depends on size. We consequently assume that the size-dependent enhanced paramagnetism diminishes at a certain temperature T_c. Hence the observed temperature dependence of magnetic susceptibility is a superposition of these contributions, χ_s and χ_{enh}, and is shown in Fig. 8. The ordinate is arbitrarily shifted in this figure. The spin susceptibility χ_s depends on temperature and decreases at about $\delta/2$ that is determined by the particle size. It is constant at higher temperatures. On the other hand, χ_{enh} decreases above T_c and probably decreases at the level of zero at infinite temperature, but it is constant below T_c. The observed temperature profile of the magnetic susceptibility, χ_g, is attributable to these two terms. It is not clear whether or not T_c depends on size. Tentatively we assume that T_c is constant at about 150 K, as the observed χ_n^s is well explained by the superposition of these terms. Three typical cases are considered. For the 5.2-nm particles δ is very small, giving $T_c \gg \delta/2$. We observe these effects being well separated at high- and low-temperature sides, as seen in Fig. 6(a). The case of the 2.5-nm particles where $T_c \sim \delta/2$ is very close to Fig. 8, which is equivalent to Fig. 6(b), except for the constant enhanced magnetism. For the 1.4-nm particles with $T_c < \delta/2$, we could no longer observe a minimum in χ_s due to the onset decrease of χ_{enh}, as shown in Fig. 6(c). The decrease of χ_{enh} at T_c does not affect Eq. (3) as stated in Sec. III. The decrement in χ_{enh} is 20% of χ_s at most, as shown in Table I, while χ_{enh} itself reaches a value five times greater than χ_s. The temperature dependence of χ_{enh} depicted in Fig. 8 is reminiscent of a phase transition for magnetism. It is necessary to measure the magnetic susceptibility at higher temperatures than in the present study in order to clarify the nature of the enhanced paramagnetism and of the phase transition. We are also carrying out experiments to observe directly and precisely the shape of Mg particles with sizes less than 2 nm.

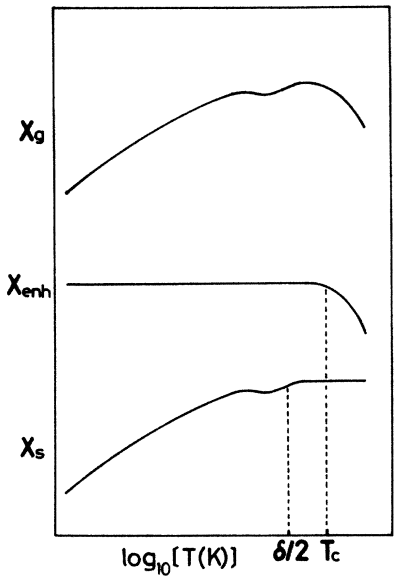

FIG. 8. Magnetic susceptibility of Mg UFP's as a function of temperature. Bottom: Spin susceptibility with noninteger exponent. The decrease of spin susceptibility is apparent at temperature $\sim\delta/2$. A minimum and a maximum are clearly seen. Middle: Enhanced paramagnetism with the transition temperature T_c. The ordinate has been arbitrarily shifted. Top: The overall magnetic susceptibility including ionic, orbital, spin, and the enhanced paramagnetism. The temperature profile of magnetic susceptibility is determined both by χ_s and χ_{enh}. The actual feature is dependent on the mutual position of $\delta/2$ and T_c. This figure corresponds approximately to the case of Fig. 6(b).

VII. SUMMARY

(1) We have observed paramagnetic enhancement in small Mg particles prepared very carefully and the enhancement is found to be proportional to the inverse of the number of atoms in a particle. This is the first discovery of zero-dimensional magnetism. The importance of the electronic state of the corner atoms of a particle is suggested. It was also suggested that the enhanced paramagnetism decreases slightly above 150 K for all particles measured. The possibility of a phase transition is proposed for this finding.

(2) After subtracting the diamagnetic susceptibility and the paramagnetic enhanced term from the observed magnetic susceptibility, we obtained the spin only magnetic susceptibility for Mg UFP with different diameters. This spin paramagnetism was well explained by the proposed formula which combines orthogonal level distribution with Poisson distribution dependent on the degree of surface roughness. The smaller the surface roughness, the closer the spin susceptibility approaches the Poisson case. In this case, the spin susceptibility slightly increases in the intermediate temperature region.

(3) The level statistics are determined and are given most approximately by the Brody distribution with the exponent $\omega \sim 0.2$. The exponent ω which characterizes the level distribution of Mg UFP's is obtained by analyzing the temperature dependence of the spin susceptibility, showing that the surface of a Mg UFP is not irregular, contrary to previous belief. This finding questions the applicability of random-matrix theory to small metal particles. This question was supported by the preliminary observation of particle shape of Mg UFP's by high-resolution electron microscope and by the recent reports on Au and Ag small particles.

ACKNOWLEDGMENTS

The authors would like to thank Dr. S. Tanaka for his invaluable discussions and suggestions. Their thanks are also due to Professor W. P. Halperin for his criticisms and suggestions. This work was supported in part by a Grant-in-Aid for Special Project Research (Grant No. 106) from the Ministry of Education, Science and Culture, Japan.

[1]R. Kubo, J. Phys. Soc. Jpn. **17**, 975 (1962).
[2]W. P. Halperin, Rev. Mod. Phys. **58**, 533 (1986).
[3]K. Kimura and S. Bandow, Phys. Rev. Lett. **58**, 1359 (1987).
[4]K. Kimura, S. Bandow, and S. Sako, Surf. Sci. **156**, 883 (1985).
[5]S. Tanaka and S. Sugano, Phys. Rev. B **34**, 740 (1986).
[6]K. Kimura and S. Bandow, Bull. Chem. Soc. Jpn. **56**, 3578 (1983).
[7]K. Kimura, Ministry of Education, Science and Culture, Japan Special Project Research No. 106, p. 115, 1985 (unpublished). The extent of particle clustering was examined through the Meissner effect of Sn superconducting small particles. For small particles, the superconducting diamagnetic susceptibility is proportional to the cubic of a diameter of particle, leading to the enormous reduction in diamagnetic susceptibility of small particles. When particle clustering takes place, the diamagnetic susceptibility is largely enhanced through a Josephson contact. We observed this enhancement in the deposited powders from solution and also in pressed discs but no enhancement was observed in the Sn particle in paraffin liquid.
[8]R. E. Cavicchi and R. H. Silsbee, Phys. Rev. Lett. **52**, 1453 (1984).
[9]K. Kimura and S. Bandow, Kotai Butsuri **20**, 467 (1984).
[10]T. Sugawara, S. Bandow, K. Kimura, H. Iwamura, and K. Itoh, J. Am. Chem. Soc. **108**, 368 (1986).
[11]*CRC Handbook of Chemistry and Physics,* edited by R. C. Weast (CRC, Boca Raton, 1981).
[12]*International Critical Tables of Numerical Data: Physics, Chemistry and Technology* (McGraw-Hill, New York, 1929), Vol. 6.
[13]H. Fröhlich, Physica **4**, 406 (1937).
[14]L. P. Gor'kov and G. M. Eliashberg, Zh. Eksp. Teor. Fiz. **48**, 1407 (1965) [Sov. Phys.—JETP **21**, 940 (1965)].
[15]R. Denton, B. Mühlschlegel, and D. J. Scalapino, Phys. Rev. B **7**, 3589 (1973).
[16]C. Kittel, *Introduction to Solid State Physics,* 2nd ed. (Wiley, New York, 1956), p. 209.
[17]S. P. Mohanty and P. K. Misra, Proc. Nucl. Phys. Solid State Phys. Symp. (India) **20C**, 437 (1977).
[18]D. C. Johnson, R. E. Benfield, P. P. Edwards, W. J. H. Nelson, and M. D. Vargas, Nature (London) **314**, 231 (1985). The crystallographic data show that the geometry of clusters is tetrahedral.
[19]S. Matsuo, J. Phys. Soc. Jpn. **44**, 1387 (1978); S. Matsuo and I. Nishida, *ibid.* **49**, 1005 (1980).
[20]H. Akoh and A. Tasaki, J. Phys. Soc. Jpn. **42**, 791 (1977).
[21]D. R. Grempel, Phys. Rev. B **24**, 3928 (1981).
[22]D. R. Grempel and S. C. Ying, Phys. Rev. Lett. **45**, 1018 (1980).
[23]M. I. Darby, Physica B + C **86-88B**, 1417 (1977).
[24]A. D. Stone, Phys. Rev. Lett. **54**, 2692 (1985).
[25]Equation (3.4) in Ref. 5 is only applicable to the two-dimensional case. Electron micrography of Mg UFP's revealed that particles were always thin plate irrespective of size and the thickness of which seemed to depend hardly on size as well. Hence we accepted, as a first approximation, the two-dimensional case rather than the three-dimensional in order to calculate the roughness parameter. If not, a slight change of parameters in the three-dimensional case leads to the same result as the two-dimensional case.
[26]S. Iijima, J. Electron Microsc. **34**, 249 (1985).
[27]T. Ichihashi, Jpn. J. Appl. Phys. **25**, 1247 (1986).